Sequential Spin-State Transition and Intermetallic Charge Transfer in $PbCoO_3$ under High Pressure

The authors report for the first time that spin-state, charge-state, crystal structure and metal-insulator transitions take place collectively in the same material system $PbCoO_3$.

Although a spin-state transition and intermetallic charge transfer have received much attention in the past, these two phenomena were never found to occur together in a particular material. $PbCoO_3$ synthesized at high pressure (12 GPa and 1323 K) provides a unique opportunity for this study by Jin-Ming Chen (NSRRC) and his international collaborators.[1] **Figure 1** shows the schematic quadruple perovskite structure of both A- and B-site-ordered $PbCoO_3$ ($Pb^{2+}Pb^{4+}{}_3Co^{2+}{}_2Co^{3+}{}_2O_{12}$) quadruple perovskite with symmetry *Pn*-3, containing corner-sharing $Co^{2+}/Co^{3+}O_6$ octahedra and isolated $Pb^{4+}O_4$ squares.

Figure 2 shows the pressure-dependent Co-Kβ X-ray emission spectra (XES) of $PbCoO_3$ measured at **SP 12U1**, a Taiwan beamline at SPring-8 in Japan. The ratio of intensity of the low-energy Kβ' line to the main emission $K\beta_{1,3}$ line is proportional to the number of unpaired electrons in the incomplete 3*d* shell and can serve to determine the spin state of Co ion as a function of temperature or pressure. With increasing pressure, the intensity of the low-energy Kβ' line decreases and almost disappears above ~15 GPa (**Fig. 2**), indicating a decreasing spin moment of Co^{2+} ion and a transition of Co^{2+} from high spin (HS) to low spin (LS). The inset of **Fig. 2** contains a plot of the integrated absolute difference (IAD) as a function of pressure; this IAD value presents a linear relation with the average spin number. In $PbCoO_3$, the total IAD changes by about 0.043 (10) with pressure increasing from 0.5 to 22.1 GPa.

Figure 3(a) shows the Co K-edge X-ray absorption spectra (XAS) of $PbCoO_3$ measured at varied pressures and normalized intensity μ = 0.8. At pressures below 15 GPa or above 30 GPa one can see a weak linear shift of the absorption edge with increasing pressure. There is an abrupt shift to higher energy from 20.2 to 29.3 GPa accompanying a variation of spectral profile, indicating the changes of valence state and crystal structure. The observed Co K-edge energy shift in $PbCoO_3$ indicates an average valence change about 0.5 (*i.e.*, from $Co^{2.5+}$ to $Co^{3.0+}$ on average), as illustrated in **Fig. 3(b)** (right scale). To fulfil the requirement of charge balance, one expects some Pb^{4+} to change to Pb^{2+} correspondingly.

Figure 3(c) presents the pressure-dependent Pb L_3-edge XAS of $PbCoO_3$. The high-resolution Pb L_3-edge partial-fluorescence-yield (PFY) XAS provides an opportunity to identify the valence state of Pb. As shown in **Fig. 3(c)**, there is a sharp shoulder S_d at lower energy, 13,030 eV, in the PFY-XAS; this feature is assigned to the dipole-allowed transition from the $2p^{3/2}$ core level to the unoccupied 6*s* states. The spectral intensity of pre-edge peak S_d represents the number of 6*s* holes and can serve to determine the valence change of Pb as a function of pressure. The spectral integral area of S_d as a function of pressure is presented in **Fig. 3(d)**. The intensity sharply decreasing with pressure increasing from 15 GPa to 30 GPa indicates the valence decrease

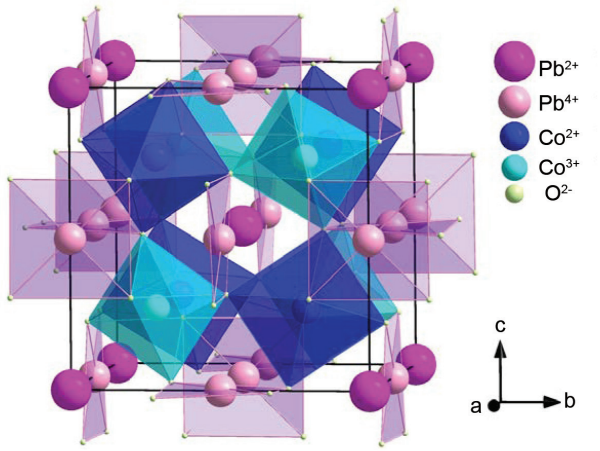

Fig. 1: Schematic crystal structure of both A- and B-site-ordered $PbCoO_3$ ($Pb^{2+}Pb^{4+}{}_3Co^{2+}{}_2Co^{3+}{}_2O_{12}$) quadruple perovskite with symmetry *Pn*-3. The corner-sharing $Co^{2+}/Co^{3+}O_6$ octahedra and isolated $Pb^{4+}O_4$ squares are shown. [Reproduced from Ref. 1]

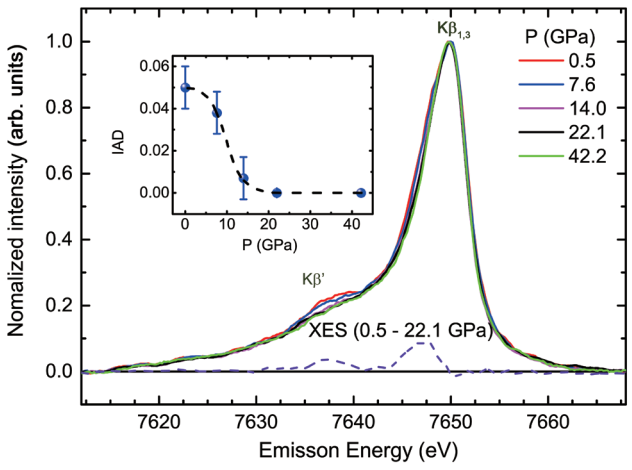

Fig. 2: Co Kβ XES of $PbCoO_3$ at varied pressures and room temperature; the inset shows the pressure dependence of IAD. [Reproduced from Ref. 1]

of Pb. Given the initial average valence state $Pb^{2+}Pb^{4+}{}_3Co^{2+}{}_2Co^{3+}{}_2O_{12}$ of $Pb^{3.5+}$ at lower pressure, the relative variation of the integral area of S_d indicates the change from $Pb^{3.5+}$ to $Pb^{3.0+}$. The Co K-edge ($Co^{2.5+}\rightarrow Co^{3.0+}$) and Pb L_3-edge ($Pb^{3.5+}\rightarrow Pb^{3.0+}$) XAS thus confirm the Pb^{4+}-Co^{2+} intermetallic charge transfer, which occurs about 15 GPa with a sharp change near 20 GPa and is complete about 30 GPa.

According to the high-pressure resistance, XES, XAS and X-ray diffraction (XRD) results, the authors obtained an interesting phase diagram of the dependence on pressure and temperature of $PbCoO_3$ as shown in **Fig. 4**.[1] i) Below ~20 GPa, the compound maintains the A- and B-site-ordered quadruple perovskite structure in cubic *Pn*-3 symmetry with charge combination $Pb^{2+}Pb^{4+}{}_3Co^{2+}{}_2Co^{3+}{}_2O_{12}$ ($Pb^{3.5+}Co^{2.5+}O_3$ on average). The HS-LS transition is expected to be complete about 15 GPa. When that spin-state transition is complete, pressure-induced intermetallic charge transfer begins between Co^{2+} and Pb^{4+} ions. ii) Between approximately 20 and 30 GPa, metallization is observed due to the accumulated effect of the Pb-Co charge transfer near 300 K, strongly indicating the melting of the ordered low-spin Co^{2+} and Co^{3+} states into mixed $Co^{2.5+}$ on average, consistent with a first-order structural phase transition to the tetra-I phase. The Pb^{4+}-Co^{2+} intermetallic charge transfer still occurs in the tetra-I phase, making the LS-Co^{2+} state become oxidized to the LS-Co^{3+} state. iii) With pressure up to ~30 GPa at 300 K, the Pb-Co intermetallic charge transfer is complete, changing the charge combination to be $Pb^{3.0+}Co^{3.0+}O_3$ on average. Because the charge transfer greatly changes the charge states and the electronic configurations for both Pb and Co ions, the compound experiences another first-order structure phase transition toward the tetra-II phase with a considerable shrinkage of volume. In the tetra-II phase, all transition-metal sites are occupied with LS-Co^{3+} with spin moment = 0. In summary, the authors present the first example in which spin-state, charge-transfer, crystal-structure and metal-insulator transitions occur collectively in the same material system, $PbCoO_3$, producing a series of intriguing variations and potential

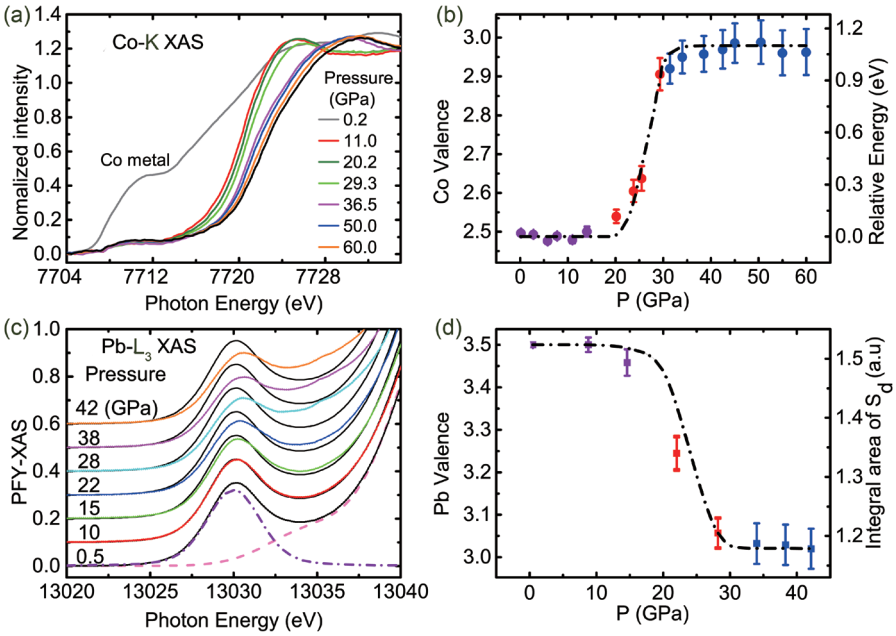

Fig. 3: XAS of $PbCoO_3$ measured at varied pressures and room temperature. (a) Co K-edge XAS at some representative pressures. (b) Relative energy shift of the Co K-edge as a function of pressure at normalized intensity μ = 0.8 after subtracting the background, and the valence-state change of Co under pressure. (c) Pre-edge peak S_d in the Pb L_3-edge PFY-XAS. For comparison, the XAS collected at 0.5 GPa is shown for data recorded at varied pressure. (d) Integral area of S_d and valence-state change of Pb as a function of pressure. The dotted and dashed curve is for visual guidance. [Reproduced from Ref. 1]

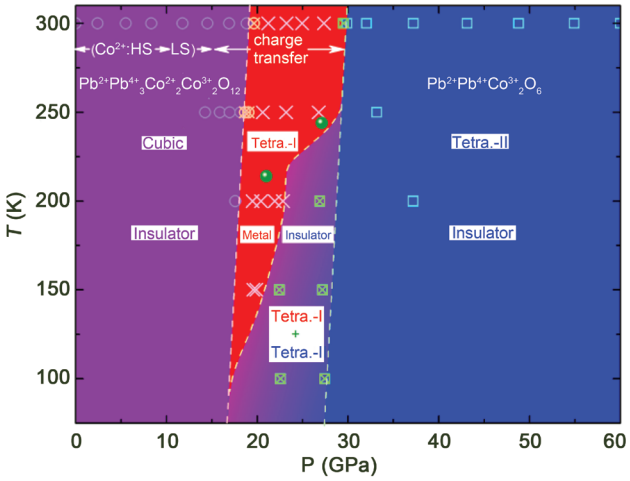

Fig. 4: Pressure- and temperature-dependent phase diagram of $PbCoO_3$. The circle (○), cross (×) and square (□) respectively stand for the cubic, tetra-I, and tetra-II phases as determined from XRD measurements. The dashed curves show the approximate phase boundaries. [Reproduced from Ref. 1]

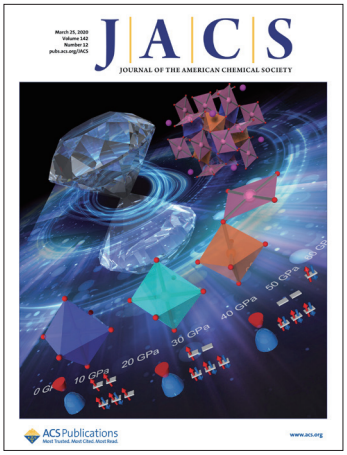

applications in lattice, charge, spin and orbital degrees of freedom. (Reported by Jin-Ming Chen)

This report features the work of Jin-Ming Chen and his collaborators published in J. Am. Chem. Soc. ***142****, 5731 (2020). This paper was selected as a cover of issue 12.*

SP 12U1 IXS

- XES, PFY-XAS
- Materials Science, Chemistry, Condensed-matter Physics

Reference

1. Z. Liu, Y. Sakai, J. Yang, W. Li, Y. Liu, X. Ye, S. Qin, J. M. Chen, S. Agrestini, K. Chen, S.-C. Liao, S.-C. Haw, F. Baudelet, H. Ishii, T. Nishikubo, H. Ishizaki, T. Yamamoto, Z. Pan, M. Fukuda, K. Ohashi, K. Matsuno, A. Machida, T. Watanuki, S. I. Kawaguchi, A. M. Arevalo-Lopez, C. Jin, Z. Hu, J. P. Attfield, M. Azuma, Y. Long, J. Am. Chem. Soc. **142**, 5731 (2020).

Hard X-ray Spectroscopy: Verification of the Active Species in Pd-Catalyzed Reactions

Rapid-scanning X-ray-absorption fine-structure spectra revealed the catalytic path of a palladium-catalysed oxidative carbonylation reaction under electrochemical conditions.

X-ray-absorption fine-structure (XAFS) spectra are widely employed in heterogeneous catalysis, materials science, physics and related disciplines for the determination of element-specific electronic and local geometric structure, but XAFS has been less commonly used for the characterization of organometallic reagents and homogeneous catalysts, especially under reaction conditions (*in situ* or *operando*).

The team of Aiwen Lei and Yi-Hung Chen (Wuhan University, China) devoted the use of the quick XAFS (QXAFS) technique at **TPS 44A** to study the structure of key intermediates (coordination, oxidation state, electronic structure and geometry) of transition-metal catalysts in cross-coupling reactions. Three key features of their projects follow. (1) The custom-made reaction cell was designed for reactions to demonstrate the laboratory procedures on the beamline. (2) Time scale ms or μs is required for the study of fractional composition of these species during experiments *in situ*. (3) QXAFS was used mainly to explore the catalytic cycles, along with various spectroscopic techniques.

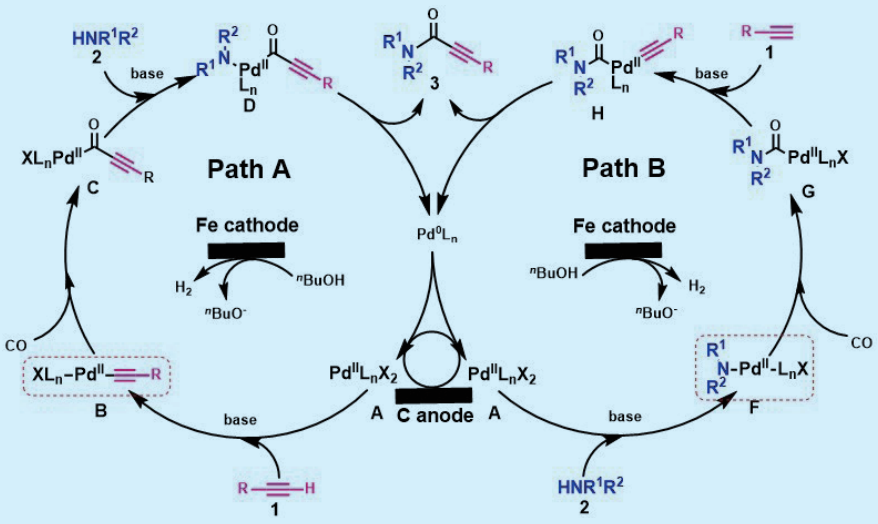

Fig. 1: Plausible reaction mechanism for electrochemical oxidative aminocarbonylation of terminal alkynes.

The detailed structural, dynamic and kinetic information (structure-reactivity relations) contributes to the theoretical basis for the optimization of a catalyst. A highly efficient catalytic system is extremely important for the environmental energy, pharmaceutical and fine chemical industry. As shown in **Fig. 1**, two possible reaction paths for the palladium-catalyzed oxidative amino-carbonylation of alkynes have been reported.[1,2] All techniques used for mechanistic studies failed to provide structural information on the metal complexes and oxidation states during the catalytic cycle.

Lei and his coworkers reported the first QXAFS scan of a solution of $Pd(OAc)_2$ and $P(p\text{-Tol})_3$ in acetonitrile that was treated with phenylacetylene, *n*-butylamine and Et_3N under a CO atmosphere. The spectrum has perfect overlap in both the X-ray absorption near-edge structure (XANES) (**Fig. 3**, blue line) and the extended X-ray-absorption fine-structure (EXAFS) spectra (**Fig. 2(a)**, blue line) with experiment *ex situ* (the solution of $Pd(OAc)_2$, $P(p\text{-Tol})_3$ and *n*-butylamine